Received: 9 & 21 October 2014

Environmental drivers of swordfish local abundance in the south-west Indian Ocean

Philippe S. Sabarros[1]*, Evgeny Romanov[2], Dominique Dagorne[3],

Loïc Le Foulgoc[2], Jean-François Ternon[4] and Pascal Bach[4]

[1]IRD, UMR 212 EME, 97420 Le Port, La Réunion

[2]CAP RUN, ARDA, 97420 Le Port, La Réunion

[3]IRD, US 191 IMAGO, 29280 Plouzané, France

[4]IRD, UMR 212 EME, CRHMT, 34203 Sète, France

*corresponding author, email: philippe.sabarros@ird.fr, tel: +262(0)693509062

ABSTRACT. Oceanic environmental conditions drive the abundance and distribution of marine organisms. Hydrodynamic structures such as fronts and eddies may become hotspots of biological activity through local concentration of nutrients. As oceanic structures generally attract forage fish and cephalopods, they often are foraging grounds for top-predators. The link between swordfish (*Xiphias gladius*) catch and environmental features in the south-west Indian Ocean is poorly documented despite Reunion Island local fishery's growing need for such information. In this study, we used a set of operational and environmental covariates to explain variations in swordfish nominal catch per unit of effort (nCPUE) throughout 2011-2013. We proceeded in two steps: (i) the nominal CPUE (nCPUE) was standardised according to operational aspects of fishing operations, and (ii) the residual CPUE (rCPUE) from the standardisation model was used to test the effects of various environmental descriptors on swordfish abundance. We found that (i) the use of circle hooks, the leader length, the number of hooks deployed and the moon phase explain 7.74% of nCPUE variations, and that (ii) the environmental model explains 19% of rCPUE. The environmental model used to predict swordfish abundance includes the effects of the seasonal Chlorophyll-a concentration trend, a latitudinal gradient, and the Eddy Kinetic Energy (EKE, derived from altimetry products) that characterises the presence of fronts and that drives local variations of swordfish abundance. Both models cumulated explain 25.92% of nCPUE variations.

KEYWORDS. Swordfish | CPUE | Environment | Longline | Reunion Island | South-west Indian Ocean

1. Introduction

Oceanic environmental conditions generally drive the abundance and distribution of marine organisms. Oceanic circulation and turbulence – from larger scales (several hundreds of kms) down to smaller scales (e.g. mesoscale, from 1-2 km to 100-200 km) – are known to drive the distribution and foraging patterns of top-predators because the probability of prey encounters is higher in and around these structures (Weimerskirch, 2007). It has been well documented that large convergence zones (e.g. polar front) correspond to foraging areas of marine birds and mammals (review by Bost et al., 2009). At smaller scales, dynamic mesoscale structures such as eddies, vertically-structured fronts and filaments are essential to the enrichment, concentration and retention of nutrients and planktonic organisms in surface waters (Bakun, 1996) which attract and shape the aggregation patterns of plankton-eaters such as small pelagic fish (Bakun, 2006; Bertrand et al., 2008; Sabarros et al., 2009). Mesoscale structures are considered as major attracting features for large predatory fish such as tuna (Young et al., 2001; Seki et al., 2002), marine mammals (Campagna et al., 2006; Cotté et al., 2007; Chaigne et al., 2012) and seabirds (Nel et al., 2001; Weimerskirch et al., 2005; Ainley et al., 2009; Hyrenbach et al., 2006).

The link between swordfish (*Xiphias gladius*) distribution and environmental features was occasionally documented in the Pacific (e.g. Bigelow et al., 1999; Seki et al., 2002; Yanez et al., 2009; Espindola et al., 2011), Atlantic (Chang et al., 2013) and there was only a few preliminary studies for the south-west Indian Ocean region where Reunion Island's longline fishing fleet targets swordfish (Guyomard et al., 2004; Sabarros et al., 2013a). It is essential to better understand the ecology and distribution patterns of swordfish in relation to oceanography in the context of an ecosystem-based management of the fishery and resource conservation.

The purpose of this study is to understand variations in catch per unit of effort (CPUE) of the main target species of pelagic longliners based in Reunion Island: swordfish using data from the self-reporting data collection program (Bach et al., 2013, Sabarros et al., 2013a, 2013b). Here, we use a novel approach consisting in two steps. First, a standardisation Generalized Additive Model (GAM) is used to remove the variations in swordfish nCPUE that can be explained by the fishing strategy and gear used. Second, an environmental GAM is used to test the effects of various environmental variables on swordfish abundance (residuals from the first model), and ultimately to predict swordfish abundance distribution.

2. Material and methods

2.1. Data

2.1.1. Swordfish data

Catch data were extracted from the Self-Reporting (SR) data collection program that is part of EU Data Collection Framework (DCF). The SR program is dedicated to monitoring captures, bycatch and depredation, and SR data can be assimilated to improved logbook type of data. SR was developed by IRD and CAP RUN and has covered since 2011 about 12% of the total fishing effort of Reunion Island semi-industrial pelagic longline fishery (Bach et al., 2013; Sabarros et al., 2013b).

In this study, we considered data between 2011 and 2013 collected on fishing boats >12 m exclusively (mini-longliners <12 m were removed from the dataset) which represent 535 monitored fishing operations. We used the nominal catch per unit of effort (nCPUE) per set, defined as the number of individuals caught per 1000 hooks, as a proxy of swordfish abundance.

2.1.2. Explanatory variables

2.1.2.1. Fishing practise and gear rigging

Fishing practise and gear are adjusted by fishermen and influence fishing performance, i.e., nCPUE. The variables describing fishing practise and gear that were available in SR are presented in Table 1. Moonlight intensity (*moon.illu*) was also included as it is tightly linked to the fishing strategy (Bach et al., 2014).

Table 1. *Operational covariates tested in the standardisation/operational model*

Covariate	Description	Unit
lightsticks_per_basket	Number of lightsticks per basket (2 or 3)	-
leader_length	Leader (or branchline) length	m
squid_bait_percent	Percent of squid bait (rest can be mackerel or others)	%
circle_hooks_percent	Percent of circle hooks (rest can be J-hooks or tuna hooks)	%
hooks_count	Total number of hooks deployed	-
depth.max	Maximum fishing depth measured on the mainline with TDR	m
moon.illu	Moonlight intensity ranging from 0 to 100	%

2.1.2.2. Environmental data

We used a set of synoptic environmental data monitored by various satellite missions: OSTIA Sea Surface Temperature (SST) provided by GHRSST (Donlon et al., 2012), Aqua-MODIS Chlorophyll-a concentration (Chla) provided by NASA (http://modis.gsfc.nasa.gov), and Sea Level Anomalies (SLA) produced by Ssalto/Duacs and distributed by AVISO with support from CNES (http://aviso.altimetry.fr). Also, we calculated descriptors of hydrographic features from AVISO altimetry-derived geostrophic currents such as the Eddy Kinetic Energy (EKE) that characterises local zones of strong current activity like meso-scale fronts for instance (Garcon et al., 2001; Zainuddin et al., 2008), and Finite-Size Lyapunov Exponents (FSLE) that describe the convergence of water masses and to some extent concentrating fronts (d'Ovidio et al., 2009). Details concerning environmental variables are provided in Table 2. Spatially-explicit environmental data were extracted within each fishing polygon and the median of the extracted distribution was retained (suffix *.med*; see Sabarros et al., 2013a). Covariates such as SST and Chla are complex as they confound seasonal, latitudinal and local components. They were therefore decomposed to segregate their respective seasonal trend component (*sst.trend*, *chl.trend*), their latitudinal component when present (*sst.lat*), and the remaining residuals corresponding to local variations (*sst.res*, *chl.res*).

Table 2. *Environmental covariates tested in the environmental model. *Calculated using AVISO altimetry-derived geostrophic currents product NRT-MSLA-UV*

Covariate	Description		Source	Unit	Spatial res.	Temporal res.
sst.trend	Sea Surface Temperature at the surface	Seasonal trend	OSTIA Level 4 composite	°C	-	Daily
sst.lat	"	Latitudinal gradient	"	"	5 km composite	"
sst.res	"	Residual SST, local variations	"	"	5 km composite	"
chl.trend	Chlorophyll-a concentration in the surface layer	Seasonal trend	MODIS Aqua Level 3	$mg.m^{-3}$	-	8 days
chl.res	"	Residual Chla, local variations	"	"	4 km composite	"
sla.med	Sea Level Anomalies : topography of the ocean, highlights meso-scale eddies	Median within a fishing polygon	AVISO NRT-MSLA-H	cm	1/3°	Daily
eke.med	Eddy Kinetic Energy : highlights frontal zones with strong currents	Median within a fishing polygon	*	$cm^2.s^{-2}$	1/3°	Daily
fsle.med	Finite-Size Lyapunov Exponent : meso-scale index of convergence of water masses	Median within a fishing polygon	*	day^{-1}	1/12°	Daily
lat	Latitude : latitudinal gradient		-	-	-	-

2.2. Statistical modelling

Data collected/extracted for each set were assumed to be independent from a set to another. We used a two-steps modelling approach (Fig. 1) that consists in using a first standardisation model on nCPUE to remove the variability that can be explained by operational aspects of fishing operations. The residual CPUE (rCPUE = residuals of the standardisation model = anomaly of CPUE) was used as a proxy of swordfish abundance in the second model to investigate the effects of environmental conditions on swordfish abundance and distribution. The two-steps modelling approach allows to predict swordfish abundance with a set of environmental variables (the ones that were selected) independently of operational aspects of fishing operations (e.g. type of boat, number of hooks deployed, fishing time, etc.). Generalized Additive Models (GAM) were used here to allow non-linear relationships and smooth terms were constrained with 4 knots to avoid overfitting.

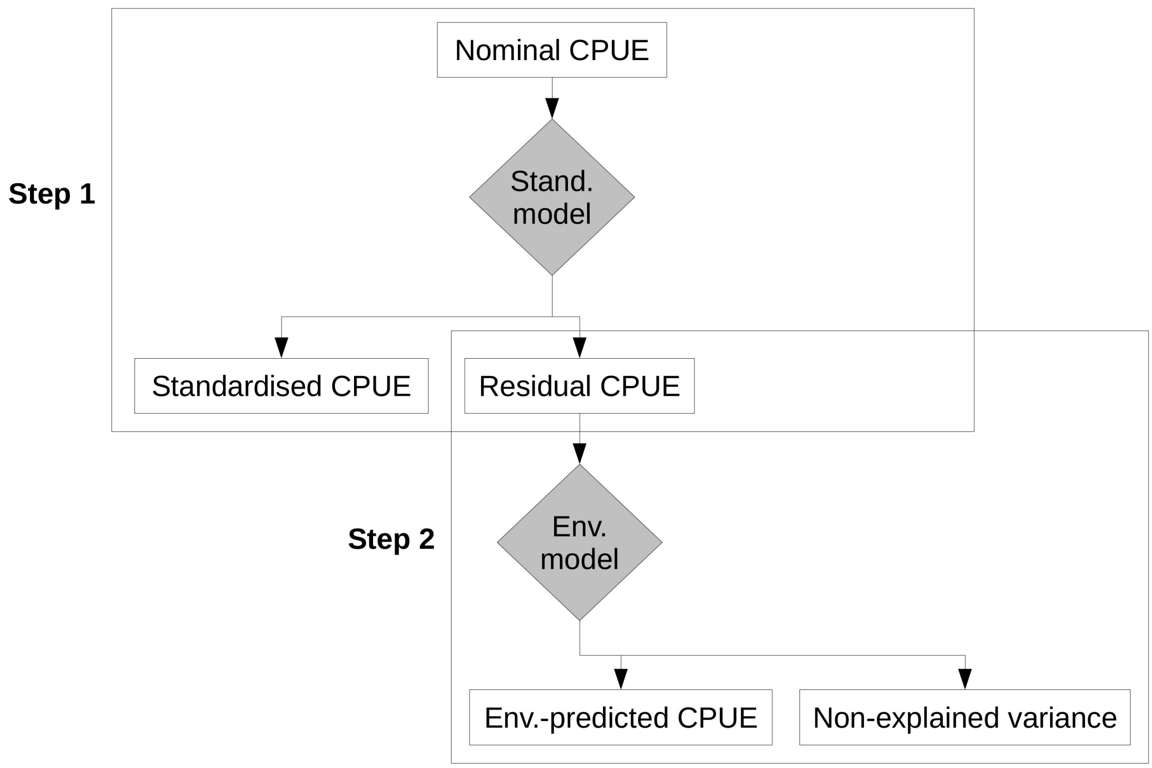

Figure 1. Two-steps modelling approach: standardisation model followed by the environmental model

2.2.1. Standardisation model

We used a GAM to explain the variations of nCPUE with operational covariates available in SR dataset (Tab. 1). The GAM was fitted with a Tweedie distribution function which is recommended for CPUE with 0 data (Candy, 2004; Coelho et al., 2014). Model selection was performed by testing all combinations of covariates and selecting the model with the lowest AICc (*pdredge* function in R package "MuMIn"; Barton, 2014). Retained covariates were checked for collinearity (not shown). The best 20 models of the 512 combinations are shown in Appendix 1.1.

2.2.2. Environmental model

Residuals from the standardisation model described above (rCPUE) were used in a GAM (Gaussian family distribution) to test for the effect of environmental covariates given in Table 2. Model selection was performed as in section 2.2.1. The 20 best models of the 256 combinations are presented in Appendix 2.1.

2.2.3. Mapped predictions

The selected environmental model was used to predict swordfish abundance (predicted anomaly of CPUE) providing a set of environmental variables. Predicted distributions were made for given dates with a spatial resolution of 1/4° and are shown for contrasted periods of the year as examples in Figure 4.

3. Results

3.1. Standardisation model

The best standardisation GAM includes 4 of the 7 tested covariates (Appendix 1.1) and explains 7.74% of the nCPUE deviance (Appendix 1.2). It includes a significant positive and asymptotic effect of the percentage of circle hooks (*circle_hook_percent*), a significant negative effect of the fishing effort in terms on number of hooks deployed (*hooks_count*), a marginal negative effect of the leader length (*leader_length*), and significant bell-shape effect of moonlight intensity (*moon.illu*) (Appendix 1.2, Fig. 2). The distribution of the model residuals using the Tweedie family link function is satisfactory (Appendix 1.2).

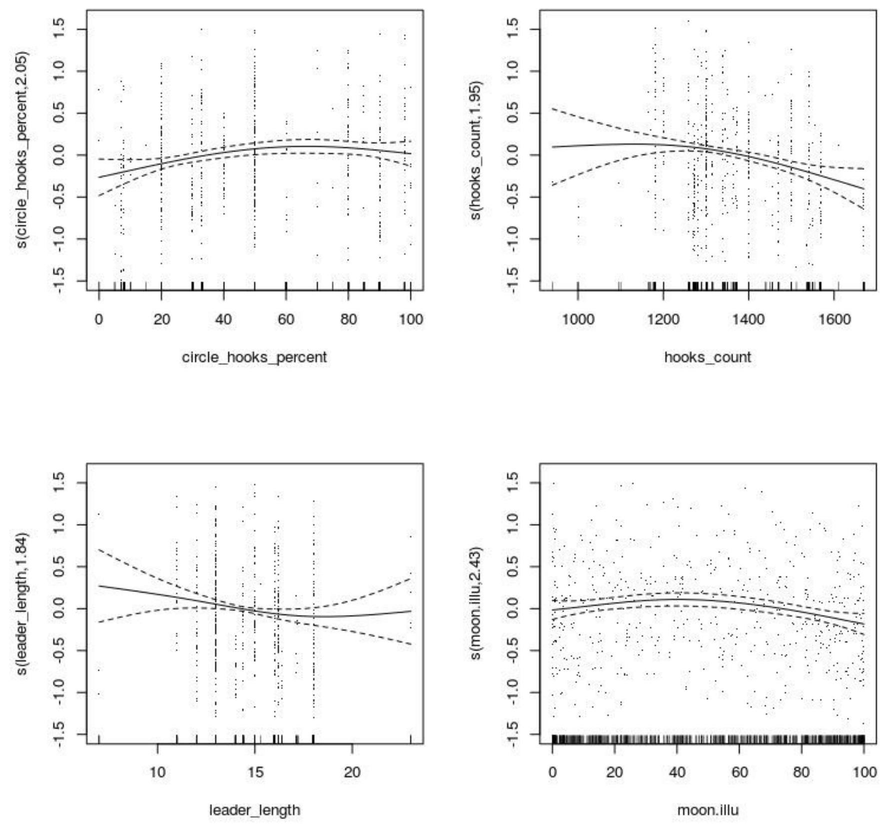

Figure 2. Smooth terms of the selected standardisation/operational model

3.2. Environmental model

Swordfish abundance (rCPUE) is driven by 3 of the 8 tested environmental covariates (Appendix 2.1). The model explains 19.7% of the deviance, which corresponds to 18.18% of the initial nCPUE variations. Both models cumulated explain 25.92% of nCPUE deviance. The environmental model includes a significant non-linear effect of the seasonal chlorophyll-a trend (*chl.trend*), a marginal (p = 0.0929) positive effect of EKE (*eke.med*), and a significant quasi-linear negative effect of the latitude (*lat*) (Appendix 2.2, Fig. 3). Residuals of the Gaussian GAM are normally distributed (Appendix 2.2).

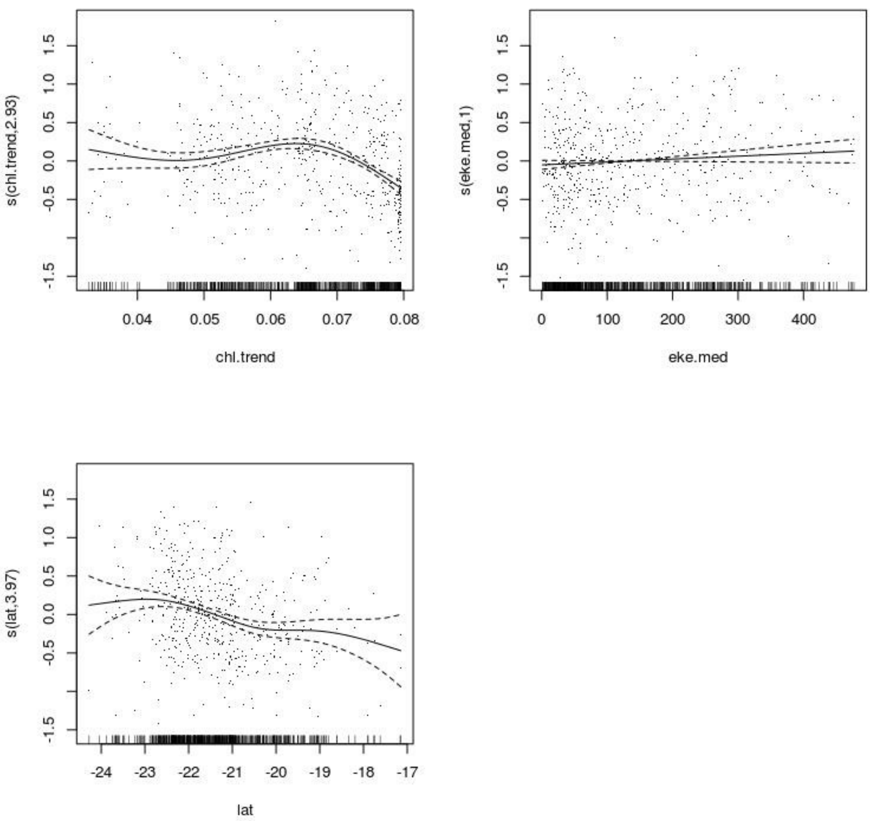

<u>Figure 3.</u> Smooth terms of the selected environmental model

3.2. Predicted swordfish distribution

Environment-driven predictions of swordfish abundance are shown in Figure 4 for contrasted seasons where swordfish mean abundance is low (June) and high (December). In the environmental model, the chlorophyll-a concentration drives the seasonal mean abundance of swordfish while EKE shapes swordfish local distribution patterns in addition to the latitudinal gradient. Stronger meso-scale activity characterised by high values of EKE, mostly occurring below 22°S, south-east coast of Madagascar and extending eastwards, is associated to local hotspots of swordfish abundance (Fig. 4) and this pattern is consistent throughout the year (Appendix 3).

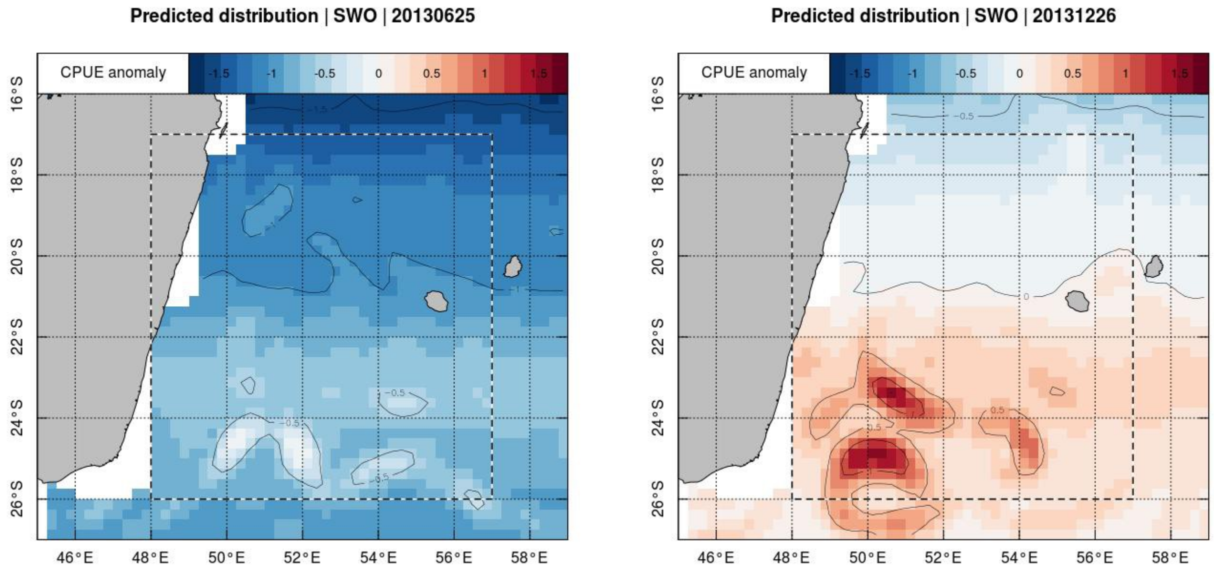

<u>Figure 4.</u> Predicted distribution of swordfish abundance (anomaly of CPUE) in low season (25-06-2013) and high season (26-12-2013). The region delimited by the dashed line corresponds to the fishing zone where SR data were collected.

4. Discussion

In the operational model that is used to standardise swordfish nCPUE, circle hooks, which are used for reducing bycatch (Favaro and Coté, 2013), catch more swordfish while it would normally be expected to slightly reduce swordfish nCPUE. Also, the length of leaders (branchlines) show here an interesting pattern: boats equipped with shorter leaders tend to capture more swordfish. The number of hooks deployed does not increase nCPUE suggesting that fishing operations with a reduced number of hooks are more efficient. Finally, nCPUE is greater during transitional moon phases while reduced around new and full moon, and this could be the consequence of a mismatch in terms of depth between the deployment of the longline and the actual swordfish distribution during the new and full moon periods (Bach et al., 2014).

In this study, both models cumulated explain a quarter of nCPUE variations (25.92%). This result is consistent with studies realised with per-set data for which deviance explained ranges between 20 and 42% (e.g., Bigelow et al., 1999; Guyomard et al., 2004; Lan et al., 2014). Other variables, that influence fishing performance (nCPUE) and that would likely increase the model prediction quality, could not be included in the models because they were not available (e.g., mixed layer depth, other environmental variables below the surface) or because they are difficult to measure (e.g., catchability).

The two-steps modelling approach is useful as this methodological framework allows to predict swordfish abundance with a model fitted on nCPUE data that have been corrected from operational effects. Predictions of swordfish abundance and distribution only necessitate a set of environmental variables, here the seasonal Chl-a trend, the latitudinal habitat gradient and the EKE.

We demonstrated here that, together with the latitudinal gradient, a local environment variable characterising meso-scale activity, namely the EKE, drives the distribution patterns of swordfish. This suggests that shearing fronts between cyclonic and anti-cylonic eddies are hydrodynamic structures that attract swordfish. Fronts, as illustrated in numbers of studies, are structures where prey availability is more predictable and that are targeted by marine top-predators (Weimerskirch, 2007; Bost et al., 2009).

Swordfish abundance is predicted to be consistently higher in the southern part of the actual fishing area (see Fig. 4). This area is characterised by a strong meso-scale dynamic patterns which extends from the south-west coast of Madagasacar towards the east. EKE reaches high values in that area and this is where the model predicts swordfish hotspots (see Fig. 4).

Finally, predicted seasonal patterns of swordfish abundance are consistent with the actual inter-annual seasonal patterns in swordfish CPUE (see Appendix 3; Sabarros et al., 2013b).

5. References

Ainley, D.G., Dugger, K.D., Ford, R.G., Pierce, S.D., Reese, D.C., Brodeur, R.D., Tynan, C.T., Barth, J.A., 2009. Association of predators and prey at frontal features in the California Current: competition, facilitation and co-occurrence. Marine Ecology Progress Series 389, 271–294. doi:10.3354/meps08153

Bach, P., Sabarros, P.S., Le Foulgoc, L., Richard, E., Lamoureux, J.P., Romanov, E., 2013. Self-reporting data collection project for the pelagic longline fishery based in La Reunion. Presented at the 9th IOTC Working Party on Ecosystems and Bycatch, La Réunion, France.

Bach, P., Sabarros, P.S., Romanov, E., Puech, A., Capello, M., Lucas, V., 2014. Patterns of swordfish capture in relation to fishing time, moon illumination and fishing depth. Presented at the 12th IOTC Working Party on Billfish, Tokyo, Japan.

Bakun, A., 1996. Patterns in the ocean. Ocean processes and marine population dynamics.

Bakun, A., 2006. Fronts and eddies as key structures in the habitat of marine fish larvae: opportunity, adaptive response and competitive advantage. Scienta Marina 70S2, 105–122.

Barton, K., 2014. MuMIn: Multi-model inference. R package version 1.10.5

Bertrand, A., Gerlotto, F., Bertrand, S., Gutiérrez, M., Alza, L., Chipollini, A., Díaz, E., Espinoza, P., Ledesma, J., Quesquén, R., Peraltilla, S., Chavez, F., 2008. Schooling behaviour and environmental forcing in relation to anchoveta distribution: An analysis across multiple spatial scales. Progress in Oceanography 79, 164–277. doi:10.1016/j.pocean.2008.10.018

Bigelow, K.A., Boggs, C.H., He, X., 1999. Environmental effects on swordfish and blue shark catch rates in the US North Pacific longline fishery. Fisheries Oceanography 8, 178–198. doi:10.1046/j.1365-2419.1999.00105.x

Bost, C.A., Cotté, C., Bailleul, F., Cherel, Y., Charassin, J.B., Guinet, C., Ainley, D.G., Weimerskirch, H., 2009. The importance of oceanographic fronts to marine birds and mammals of the southern oceans. Journal of Marine Systems 78, 363–376. doi:10.1016/j.jmarsys.2008.11.022

Campagna, C., Piola, A.R., Rosa_Marin, M., Lewis, M., Fernández, T., 2006. Soutern elephant seal trajectories, fronts and eddies in the Brazil/Malvinas Confluence. Deep-Sea Research I 53, 1907–1924. doi:10.1016/j.dsr.2006.08.015

Candy, S.G., 2004. Modelling catch and effort data using generalised linear models, the Tweedie distribution, random vessel effects and random stratum-by-year effects. Ccamlr Science 11, 59–80.

Chaigne, A., Authier, M., Richard, P., Cherel, Y., Guinet, C., 2013. Shift in foraging grounds and diet broadening during ontogeny in southern elephant seals from Kerguelen Islands. Marine Biology 160, 977–986. doi:10.1007/s00227-012-2149-5

Chang, Y.-J., Sun, C.-L., Chen, Y., Yeh, S.-Z., DiNardo, G., Su, N.-J., 2013. Modelling the impacts of environmental variation on the habitat suitability of swordfish, Xiphias gladius, in the equatorial Atlantic Ocean. ICES Journal of Marine Science 70, 1000–1012. doi:10.1093/icesjms/fss190

Coelho, R., Nikolic, N., Evano, H., Miguel, N., Bourjea, J., others, 2014. Reunion island pelagic longline fishery characterization and standardization of albacore catch rates, in: IOTC.

Cotté, C., Park, Y.H., Guinet, C., Bost, C.A., 2007. Movements of foraging king penguins through marine mesoscale eddies. Proceedings of the Royal Society B 274, 2385–2391. doi:10.1098/rspb.2007.0775

Donlon, C.J., Martin, M., Stark, J., Roberts-Jones, J., Fiedler, E., Wimmer, W., 2012. The Operational Sea Surface Temperature and Sea Ice Analysis (OSTIA) system. Remote Sensing of Environment 116, 140–158. doi:10.1016/j.rse.2010.10.017

D’Ovidio, F., Isern-Fontanet, J., López, C., Hernández-García, E., García-Ladona, E., 2009.

Comparison between Eulerian diagnostics and finite-size Lyapunov exponents computed from altimetry in the Algerian basin. Deep Sea Research Part I: Oceanographic Research Papers 56, 15–31. doi:10.1016/j.dsr.2008.07.014

Espíndola, F., Yáñez, E., Barbieri, M.Á., 2011. El Niño Southern Oscillation and spatial-temporal variability of the nominal performances of swordfish (Xiphias gladius) in the southeastern Pacific. Rev. biol. mar. oceanogr 46, 231–242.

Favaro, B., Côté, I.M., 2013. Do by-catch reduction devices in longline fisheries reduce capture of sharks and rays? A global meta-analysis. Fish and Fisheries. doi:10.1111/faf.12055

Garçon, V.C., Oschlies, A., Doney, S.C., McGillicuddy, D., Waniek, J., 2001. The role of mesoscale variability on plankton dynamics in the North Atlantic. Deep Sea Research Part II: Topical Studies in Oceanography 48, 2199–2226.

Guyomard, D., Desruisseaux, M., Poisson, F., Taquet, M., Petit, M., 2004. GAM analysis of operational and environmental factors affecting swordfish (Xiphias gladius) catch and CPUE of the Reunion Island longline fishery, in the South Western Indian Ocean, in: 4ème Session Du Groupe de Travail de La CTOI Sur Les Poissons Porte-Épée, 27 Septembre-1er Octobre 2004, Maurice.

Hyrenbach, K.D., Veit, R.R., Weimerskirch, H., Hunt, G.L., 2006. Seabird associations with mesoscale eddies: the subtropical Indian Ocean. Marine Ecology Progress Series 324, 271–279.

Lan, K.-W., Lee, M.-A., Wang, S.-P., Chen, Z.-Y., 2014. Environmental variations on swordfish (Xiphias gladius) catch rates in the Indian Ocean. Fisheries Research. doi:10.1016/j.fishres.2014.08.010

Nel, D.C., Lutjeharms, J.R.E., Pakhomov, E.A., Ansorge, I.J., Ryan, P.G., Klages, N.T.W., 2001. Exploitation of mesoscale oceanographic features by grey-headed albatross Thalassarche chrysostoma in the southern Indian Ocean. Marine Ecology Progress Series 217, 15–26.

Poisson, F., Gaertner, J.-C., Taquet, M., Durbec, J.-P., Bigelow, K., 2010. Effects of lunar cycle and fishing operations on longline-caught pelagic fish: fishing performance, capture time, and survival of fish. Fishery Bulletin 108, 268–281.Sabarros, P.S., Ménard, F., Lévénez, J.-J., Tew-Kai, E., Ternon, J.-F., 2009. Mesoscale eddies influence distribution and aggregation patterns of micronekton in the Mozambique Channel. Marine Ecology Progress Series 395, 101–107. doi:10.3354/meps08087

Sabarros, P.S., Romanov, E., Le Foulgoc, L., Richard, E., Dagorne, D., Bach, P., 2013a. Exploratory analysis of relationships between swordfish captures and environmental features in the southwest Indian Ocean. Presented at the 11th IOTC Working Party on Billfish, La Réunion, France.

Sabarros, P.S., Romanov, E., Le Foulgoc, L., Richard, E., Lamoureux, J.P., Bach, P., 2013b.

Commercial catch and discards of pelagic longline fishery of Reunion Island based on the self-reporting data collection program. Presented at the 9th IOTC Working Party on Ecosystems and Bycatch, La Réunion, France.

Seki, M.P., Polovina, J.J., Kobayashi, D.R., Bidigare, R.R., Mitchum, G.T., 2002. An oceanographic characterization of swordfish (Xiphias gladius) longline fishing grounds in the springtime subtropical North Pacific. Fisheries Oceanography 11, 251–266.

Weimerskirch, H., 2007. Are seabirds foraging for unpredictable resources? Deep-Sea Research II 54, 211–223. doi:10.1016/j.dsr2.2006.11.013

Weimerskirch, H., Le Corre, M., Jaquemet, S., Marsac, F., 2005. Foraging strategy of a tropical seabird, the red-footed booby, in a dynamic marine environment. Marine Ecology Progress Series 288, 251–261.

Yáñez, E., 2009. Environmental conditions associated with swordfish size compositions and catches off the Chilean coast. Latin American Journal of Aquatic Research 37, 71–81. doi:10.3856/vol37-issue1-fulltext-6

Young, J.W., Bradford, R., Lamb, T.D., Clementson, L.A., Kloser, R., Galea, H., 2001. Yellowfin tuna (Thunnus albacares) aggregations along the shelf break off south-eastern Australia: links between inshore and offshore processes. Marine and Freshwater Research 52, 463–474.

Zainuddin, M., Saitoh, K., Saitoh, S.-I., 2008. Albacore (Thunnus alalunga) fishing ground in relation to oceanographic conditions in the western North Pacific Ocean using remotely sensed satellite data. Fisheries Oceanography 17, 61–73. doi:10.1111/j.1365-2419.2008.00461.x

6. Aknowledgements

We thank EU FEP (Fonds Européens pour la Pêche) from supporting IRD and CAP RUN research programs PROSPER 1 and 2, and EU DCF (Data Collection Framework) for supporting the Self-Reporting data collection program.

7. Appendices

<u>Appendix 1.1.</u> *Twenty best standardisation/operation models of the model selection procedure. "+" indicates that the covariate is included in the model. The first model with the lowest AICc is the selected model.*

rank	(Intercept)	lightsticks_count_by_basket	s(circle_hooks_percent, k = 4)	s(depth.max, k = 4)	s(hooks_count, k = 4)	s(leader_length, k = 4)	s(moon.illu)	s(squid_bait_percent, k = 4)	df	logLik	AICc	delta	weight
1	1,53	NA	+	NA	+	+	+	NA	13,08	-1288,23	2603,33	0,00	0,09
2	1,53	NA	+	+	+	NA	+	NA	11,57	-1290,20	2604,10	0,77	0,06
3	1,53	NA	+	+	+	+	+	+	15,71	-1285,88	2604,19	0,86	0,06
4	1,53	NA	+	NA	+	+	+	+	13,99	-1287,72	2604,24	0,91	0,06
5	1,53	NA	+	NA	+	NA	+	NA	10,12	-1291,83	2604,33	1,00	0,06
6	1,53	NA	+	+	+	+	+	NA	14,94	-1286,82	2604,43	1,10	0,05
7	1,53	NA	+	+	+	NA	+	+	13,02	-1288,85	2604,43	1,10	0,05
8	1,50	+	+	NA	+	+	+	NA	14,28	-1287,61	2604,62	1,29	0,05
9	1,53	NA	NA	+	+	NA	+	+	12,32	-1289,84	2604,94	1,61	0,04
10	1,48	+	+	+	+	+	+	+	17,33	-1284,59	2605,07	1,74	0,04
11	1,49	+	+	+	+	+	+	NA	16,20	-1285,95	2605,38	2,05	0,03
12	1,53	NA	+	NA	+	NA	+	+	11,46	-1290,98	2605,43	2,10	0,03
13	1,51	+	+	+	+	NA	+	NA	12,46	-1289,97	2605,50	2,17	0,03
14	1,53	NA	NA	+	+	+	+	+	13,34	-1289,13	2605,68	2,35	0,03
15	1,50	+	+	+	+	NA	+	+	13,98	-1288,48	2605,73	2,40	0,03
16	1,50	+	+	NA	+	+	+	+	15,69	-1286,75	2605,89	2,56	0,03
17	1,53	NA	NA	NA	+	NA	+	+	11,25	-1291,47	2605,97	2,65	0,02
18	1,53	NA	NA	NA	+	+	+	+	12,82	-1289,88	2606,07	2,74	0,02
19	1,52	+	+	NA	+	NA	+	NA	11,04	-1291,80	2606,18	2,85	0,02
20	1,52	+	NA	+	+	NA	+	+	13,38	-1289,52	2606,53	3,20	0,02

Appendix 1.2. Details of the selected standardisation/operational GAM and model fitting diagnostics

```
Family: Tweedie(p=1.162)
Link function: log

Formula:
cpue ~ s(circle_hooks_percent, k = 4) + s(hooks_count, k = 4) +
    s(leader_length, k = 4) + s(moon.illu) + 1

Parametric coefficients:
            Estimate Std. Error t value Pr(>|t|)
(Intercept)  1.53155    0.02675   57.25   <2e-16 ***
---
Signif. codes:  0 '***' 0.001 '**' 0.01 '*' 0.05 '.' 0.1 ' ' 1

Approximate significance of smooth terms:
                          edf Ref.df     F  p-value
s(circle_hooks_percent) 2.053  2.429 4.402 0.008776 **
s(hooks_count)          1.951  2.368 8.043 0.000184 ***
s(leader_length)        1.845  2.278 2.168 0.107054
s(moon.illu)            2.428  3.006 3.881 0.009154 **
---
Signif. codes:  0 '***' 0.001 '**' 0.01 '*' 0.05 '.' 0.1 ' ' 1

R-sq.(adj) =  0.0676   Deviance explained = 7.74%
-REML = 1304.4  Scale est. = 1.3695    n = 535
```

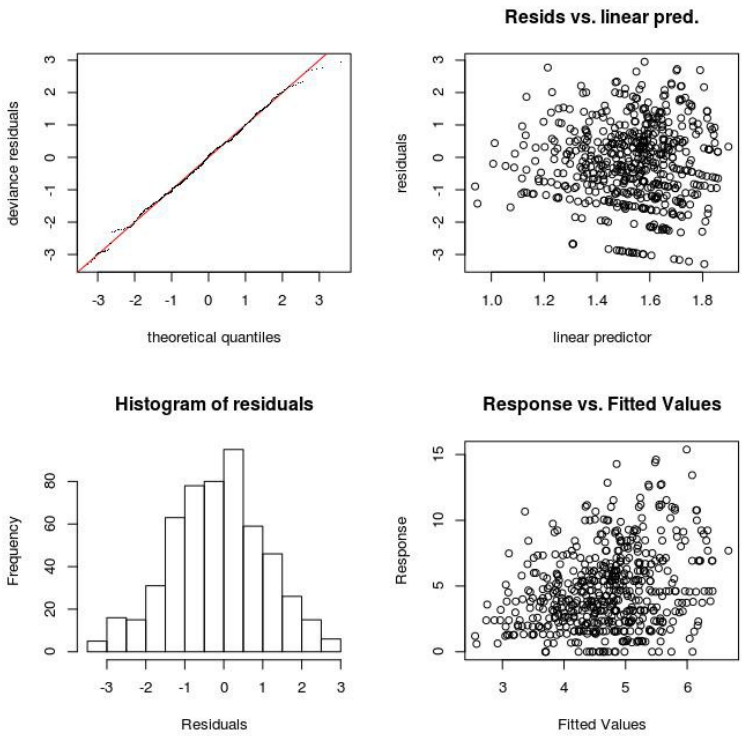

<u>Appendix 2.1.</u> *Twenty best environmental models in the model selection procedure. "+" indicates that the covariate is included in the model. The first model with the lowest AICc is the selected model.*

rank	(Intercept)	s(chl.res, k = 4)	s(chl.trend, k = 4)	s(eke.med, k = 4)	s(fsle.med, k = 4)	s(lat)	s(sla.med, k = 4)	s(sst.res, k = 4)	s(sst.trend, k = 4)	df	logLik	AICc	delta	weight
1	-0,06	NA	+	+	NA	+	NA	NA	NA	9,90	-409,23	838,68	0,00	0,06
2	-0,06	NA	+	+	NA	+	NA	NA	+	10,43	-408,71	838,74	0,06	0,06
3	-0,06	+	+	+	NA	+	NA	NA	NA	11,40	-407,76	838,88	0,20	0,05
4	-0,06	NA	+	NA	NA	+	NA	NA	+	9,50	-409,84	839,07	0,39	0,05
5	-0,06	NA	+	NA	NA	+	NA	NA	NA	9,05	-410,45	839,37	0,69	0,04
6	-0,06	+	+	NA	NA	+	NA	NA	NA	10,56	-408,94	839,47	0,79	0,04
7	-0,06	+	+	+	NA	+	NA	NA	+	11,97	-407,73	840,02	1,34	0,03
8	-0,06	NA	+	+	NA	+	+	NA	+	11,49	-408,25	840,05	1,36	0,03
9	-0,06	NA	+	+	+	+	NA	NA	NA	10,88	-408,98	840,23	1,55	0,03
10	-0,06	+	+	NA	NA	+	NA	NA	+	11,06	-408,86	840,37	1,69	0,03
11	-0,06	+	+	+	+	+	NA	NA	NA	12,37	-407,57	840,53	1,85	0,02
12	-0,06	NA	+	+	+	+	NA	NA	+	11,44	-408,56	840,55	1,87	0,02
13	-0,06	+	+	+	NA	+	NA	+	NA	12,51	-407,45	840,60	1,92	0,02
14	-0,06	NA	+	+	NA	+	+	NA	NA	10,95	-409,12	840,64	1,96	0,02
15	-0,06	NA	+	NA	NA	+	+	NA	+	10,77	-409,32	840,67	1,99	0,02
16	-0,06	NA	+	+	NA	+	NA	+	NA	10,90	-409,22	840,75	2,06	0,02
17	-0,06	NA	+	NA	+	+	NA	NA	NA	10,03	-410,14	840,77	2,09	0,02
18	-0,06	NA	+	NA	+	+	NA	NA	+	10,51	-409,65	840,80	2,11	0,02
19	-0,06	NA	+	+	NA	+	NA	+	+	11,49	-408,64	840,83	2,14	0,02
20	-0,06	+	+	+	NA	+	+	NA	NA	12,42	-407,68	840,88	2,19	0,02

Appendix 2.2. Details of the selected environmental GAM and model fitting diagnostics.

```
Family: gaussian
Link function: identity

Formula:
cpueres ~ s(chl.trend, k = 4) + s(eke.med, k = 4) + s(lat) +
    1

Parametric coefficients:
            Estimate Std. Error t value Pr(>|t|)
(Intercept) -0.05735    0.02347  -2.444   0.0149 *
---
Signif. codes:  0 '***' 0.001 '**' 0.01 '*' 0.05 '.' 0.1 ' ' 1

Approximate significance of smooth terms:
               edf Ref.df      F  p-value
s(chl.trend) 2.931  2.996 21.135 5.87e-13 ***
s(eke.med)   1.000  1.000  2.833   0.0929 .
s(lat)       3.967  4.939  6.674 5.77e-06 ***
---
Signif. codes:  0 '***' 0.001 '**' 0.01 '*' 0.05 '.' 0.1 ' ' 1

R-sq.(adj) =  0.177   Deviance explained =   19%
GCV = 0.29135  Scale est. = 0.28636   n = 520
```

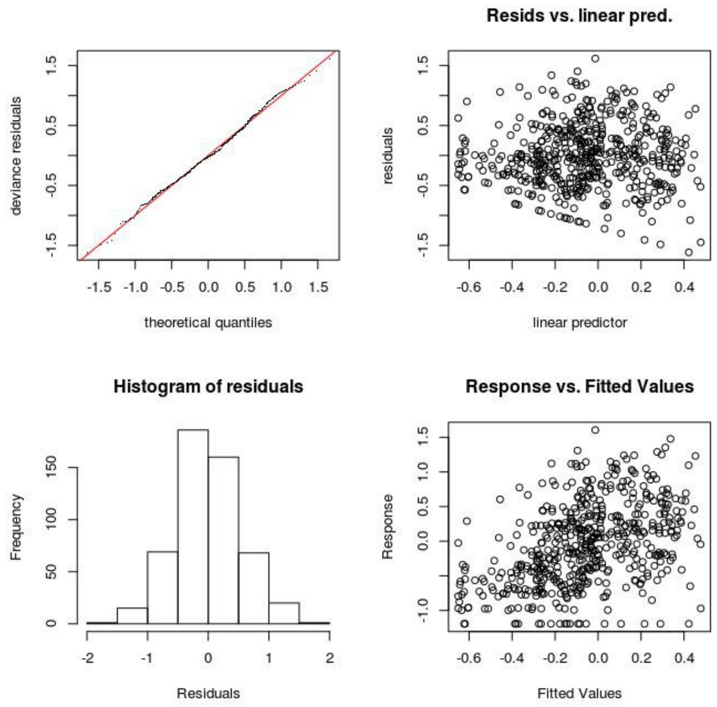

Appendix 3. Monthly snapshots of swordfish predicted distribution in 2013.